High Reuse Efficiency of Radio Resources in Urban Microcellular Systems

Ho-Shin Cho, *Member, IEEE*, Jae Kyun Kwon, *Student Member, IEEE*, and Dan Keun Sung, *Member, IEEE*

***Abstract*—A new microcell configuration scheme in urban areas is proposed in order to increase the reuse efficiency of radio resources. Multiple directional-beam antennas lined up along a street form a cigar-shaped cell. Antennas are located at intersection and are directed along the intersecting streets. Two antennas facing each other form a microzone and, therefore, a cigar-shaped cell consists of multiple microzones in a line. Each microzone is protected against cochannel interference from neighboring microzones by confinement of transmitted signals to a microzone using down-tilting of antenna beams. Therefore, a radio channel which is occupied in one microzone can be used in adjacent microzones. An increase in system capacity is achieved by the high reuse efficiency of radio resources. The proposed system increases system capacity up to 560% with a call blocking probability of 1% when compared with a conventional system. In addition, a macrodiversity scheme using two antennas in a microzone improves call quality on reverse link.**

***Index Terms*—Antenna beam tilting, cigar-shaped cell, directional-beam antenna, reuse efficiency.**

I. Introduction

DEMANDS on multimedia services including voice, data, and video have grown rapidly in wireless communication networks. In order to cope with the various demands, future wireless communication systems will require a large capacity.

System capacity can be increased by augmenting the reuse efficiency of limited radio resources. As a solution to this problem, many types of dynamic channel assignment (DCA) scheme have been investigated [1]–[3]. In general, DCA schemes have some degree of flexibility for channel reuse subject to cochannel interference constraints, thereby adaptively improving the radio resource efficiency against traffic variation. Employing antenna techniques, Pan *et al.* [4] and Cho *et al.* [5] considered sectorized multibeam cellular systems with DCA. However, the performance improvement of DCA schemes costs system complexity.

As another solution, microcellular systems with low transmitting power base stations (BSs) have been proposed in order to increase the reuse efficiency [6], [7]. However, such low-power systems require a large number of BSs and generate frequent intercell handoffs. Fiber-optic microcellular systems integrated with technologies such as subcarrier multiplexing (SCM) and spectrum delivery switching (SDS) have been proposed and extensively investigated for implementation of low cost, small-sized BSs [8]–[10]. Cho *et al.* [11] proposed a movable safety zone scheme which assigns a radio channel to multiple users within a cell and, therefore, increases the radio channel reuse efficiency using a fiber-optic microcellular technology.

A new microcell configuration in urban areas is proposed in order to increase the reuse efficiency of radio resources. Multiple directional-beam antennas lined up along a street form a cigar-shaped cell. Antennas are located at the intersection and are directed along the intersecting streets. Two antennas facing each other form a microzone and the resulting cigar-shaped cell consists of multiple microzones in a line. Each microzone is protected against cochannel interference from neighboring microzones by confinement of transmitted signals to a microzone using down-tilting of antenna beams [12], [13]. Therefore, a radio channel which is occupied in one microzone can be used in adjacent microzones. High efficiency achieved through channel reusing increases system capacity. In addition, a macrodiversity scheme using two antennas in a microzone improves call quality on reverse link.

The proposed system is analyzed using an $M/G/N$ loss model which includes: 1) a Poisson distribution of call arrivals, [**M**emoryless property of interarrival time]; 2) a **G**enerally distributed call service time; 3) a finite system capacity with **N** servers; and 4) a blocked system (call **loss**). Low-tier user mobility features in urban areas, such as walking along a street and turning at an intersection, are considered using the framework developed in [14]. The system is evaluated using numerical examples obtained by an iteration method in terms of blocking and forced dropping probabilities, and the handoff call arrival rate.

This paper is organized as follows: in Section II a microcell configuration consisting of microzones is proposed and the management of microzones and traffic channels is described. In Section III the performance of the proposed system is evaluated. In Section IV numerical examples are given to illustrate the blocking and dropping probabilities, the handoff call arrival rate, and the reuse efficiency. Conclusions are presented in Section V.

II. System Description

A. Microcell Configuration

Fig. 1 illustrates a microcell configuration. A grid-structured urban area with horizontal and vertical streets is considered. Four directional narrow-beam antennas are located at each intersection and are directed along the intersecting streets. Two directional-beam antennas facing each other form a microzone

Manuscript received January 14, 1999; revised January 11, 2000.

H.-S. Cho was with the Department of Electrical Engineering, Korea Advanced Institute of Science and Technology, Taejon, Korea. He is now with the Electronics and Telecommunications Research Institute, Taejon, Korea (e-mail: chohs@etri.re.kr).

J. K. Kwon and D. K. Sung are with the Department of Electrical Engineering, Korea Advanced Institute of Science and Technology, Taejon, Korea (e-mail: jack@cnr.kaist.ac.kr; dksung@ee.kaist.ac.kr).

Publisher Item Identifier S 0018-9545(00)07921-4.

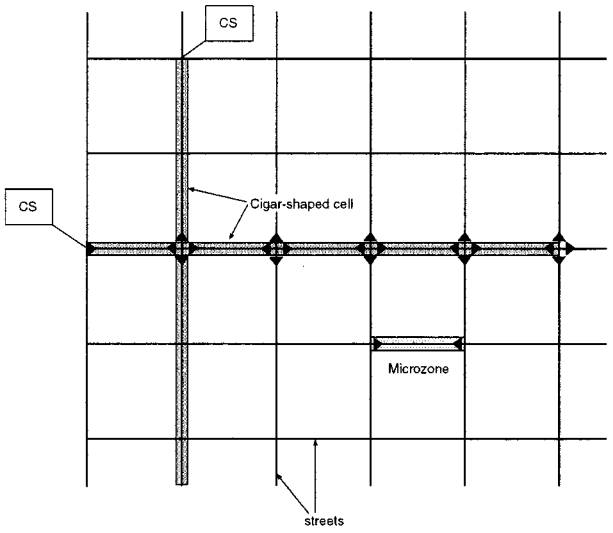

Fig. 1. A microcell configuration.

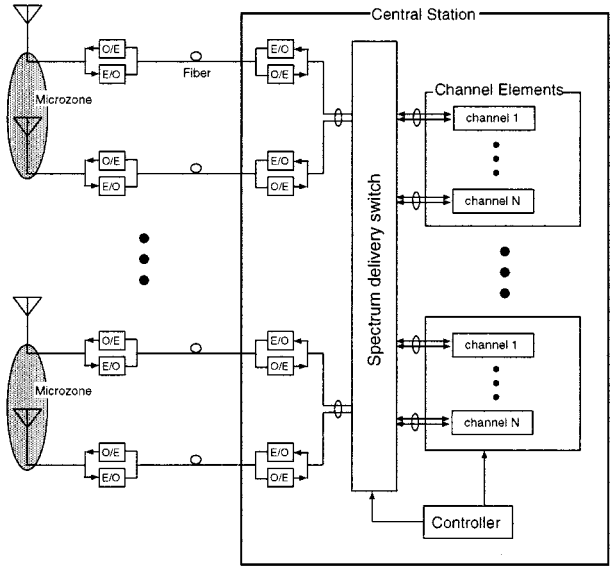

Fig. 2. Block diagram of the proposed system.

which corresponds to a street block. A cigar-shaped urban cell consists of multiple microzones in a line. This system uses the fiber-optic microcell configuration shown in Fig. 2. A large number of antenna ports are implemented at low cost by installation of all channel elements in a central station (CS). Messages between antenna ports and CS are transmitted by subcarrier multiplexing (SCM) [15] and traffic channels are dynamically assigned according to traffic demand in each microzone by spectrum delivery switching (SDS) [16].

B. Management of Noninterfered Microzones

Directional beam antennas are tilted downward to effectively confine transmitted signals to each microzone, thereby protecting users against cochannel interference from neighboring microzones. The BS transmission power and beam-tilting angle are controlled so that the coverage of one directional antenna cannot reach the opposite end of a microzone, as shown in Fig. 3. This narrow coverage gives users more effective protection against cochannel interference from neighboring microzones and allows simultaneous radio channel use in adjacent microzones (see the interference analysis in the Appendix). The coverage of two microzone antennas overlaps. On reverse link, two uncorrelated fading signals are available to the users staying in the overlapping area by using two separated microzone antennas. Therefore, macrodiversity schemes can be employed by combining the separately demodulated signals in a channel element including two modems. On the other hand, only one microzone antenna and one modem are used on forward link. An antenna switching between the two microzone antennas is done in the overlapping area.

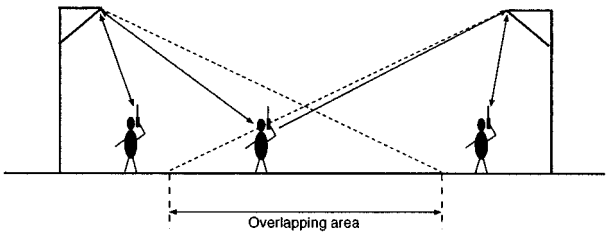

Fig. 3. Management of call connections to directional beam antennas in a microzone.

C. Traffic Channel and Call Management Scheme

A CS needs to manage multiple identical traffic channel sets each of which has N channel elements. A channel set is expressed as

$$C = \{c_1 \quad c_2 \quad \cdots \quad c_N\}. \tag{1}$$

A channel c_i, $i = 1, 2, \ldots, N$, can be used commonly in multiple microzones at the same time. The utility index ϕ of a microzone is defined as

$$\phi(c_i) = \begin{cases} 0, & \text{if } c_i \text{ is idle} \\ 1, & \text{if } c_i \text{ is busy} \end{cases} \tag{2}$$

and the reuse index $\eta(c_i)$ represents how many microzones are using the channel c_i in a cigar-shaped cell. Let γ denote the number of channel sets installed in CS. Then, $\eta(c_i)$ is given by

$$0 \le \eta(c_i) \le \gamma, \qquad \text{for } 0 \le i \le N. \tag{3}$$

For a given microzone an available channel set is defined as

$$C_A = \{c_i | \phi(c_i) = 0 \text{ and } \eta(c_i) < \gamma \text{ for } 0 \le i \le N\}. \tag{4}$$

If C_A is an empty set, i.e., $C_A = \emptyset$, a new call is blocked.

A handoff call is requested when a caller leaves the current cell and enters a neighboring cell either through a right-angle turn at an intersection or by crossing a cell boundary. On the other hand, when a caller moves to a new microzone within a cell, which is called an *intracell migration*, the caller can hold the current channel c_i by simple antenna switching at the CS if $\phi(c_i) = 0$ in the target microzone. However, if $\phi(c_i) = 1$, the caller is assigned a new available channel c_j such that $c_j \in C_A$ in the target microzone. This type of handoff is called an intracell handoff. If $C_A = \emptyset$ in the target microzone the call is terminated.

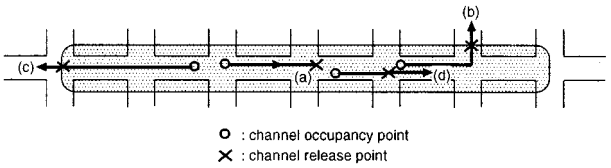

Fig. 4. Four cases of channel releases.

III. Performance Evaluation

In order to evaluate the performance of the proposed system the following definitions and assumptions are made.

- New calls are uniformly distributed in a cell and follow a Poisson process with a rate of λ_n.
- The call holding time T_{ch} is exponentially distributed with a mean of $1/\mu_{ch}$.
- The microzone dwelling time $T_{dw}^{(i)}$ is defined as the time duration from the instant that a user generates a call to the instant that the user leaves the ith microzone from the home microzone.
- $T_{dw}^{(i)}$ has an ir-stage Erlang distribution with a mean of i/μ_{dw} with a probability density function given by

$$f_{T_{dw}^{(i)}}(t) = \frac{r\mu_{dw}(r\mu_{dw}t)^{ir-1}}{(ir-1)!}\exp(-r\mu_{dw}t). \tag{5}$$

A. Channel Holding Time

The channel holding time T_{cho} is the time duration between channel occupancy and channel release. Fig. 4 shows four cases of channel release: (a) a caller completes the call; (b) a caller turns at an intersection (a turning handoff); (c) a caller crosses a cell boundary (a straight handoff); and (d) a caller needs an intracell handoff. Let T_t, T_s and T_{ih} denote the time duration between a channel occupancy and turning at an intersection, straight crossing of a cell boundary, and intracell handoff, respectively. Then, T_{cho} is expressed as

$$T_{cho} = \min(T_{ch}, T_t, T_s, T_{ih}). \tag{6}$$

Since, in the proposed system, T_{ih} is expected to be much larger than other variables, T_{ch}, T_t, and T_s, (6) can be approximated as

$$T_{cho} \approx \min(T_{ch}, T_t, T_s). \tag{7}$$

This approximation will be justified by simulation later in this section.

Let m_t and m_s denote the number of microzones through which a user passes before turning at an intersection and a straight crossing of a cell boundary, respectively. Then, the cumulative distribution function of T_t is obtained as

$$\begin{aligned} F_{T_t}(t) &= 1 - \Pr(T_t > t) \\ &= 1 - \sum_{i=1}^{\infty} \Pr(T_t > t | m_t = i)\Pr(m_t = i) \\ &= 1 - \sum_{i=1}^{\infty} \Pr\left(T_{dw}^{(i)} > t\right) P_s^{i-1}(1-P_s) \end{aligned} \tag{8}$$

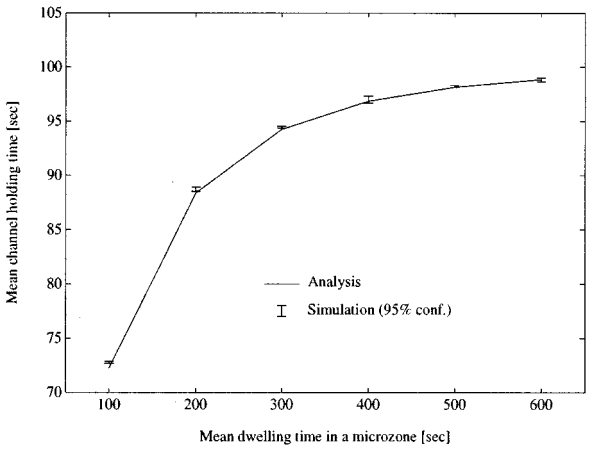

Fig. 5. Comparison between analytical results and simulation for $E[T_{ch}] = 100$ s, $M = 10$, $P_s = 0.5$, and $r = 5$.

where P_s is the probability of straight movement (not turning at intersections). Using (5) and (8) yields

$$\begin{aligned} F_{T_t}(t) = 1 - \exp(-r\mu_{dw}t)(1-P_s) \sum_{i=1}^{\infty} P_s^{i-1} \\ \times \sum_{n=0}^{ir-1} \frac{(r\mu_{dw}t)^n}{n!}. \end{aligned} \tag{9}$$

Similarly, the cumulative distribution function of T_s is derived as

$$\begin{aligned} F_{T_s}(t) &= 1 - \Pr(T_s > t) \\ &= 1 - \sum_{i=1}^{M} \Pr(T_s > t | m_s = i)\Pr(m_s = i) \\ &= 1 - \frac{\exp(-r\mu_{dw}t)}{M} \sum_{i=1}^{M} \sum_{n=0}^{ir-1} \frac{(r\mu_{dw}t)^n}{n!} \end{aligned} \tag{10}$$

where M is the number of microzones in a cell. From the three cumulative distribution functions of T_{ch}, T_t, and T_s, the cumulative distribution function of T_{cho} is obtained as

$$\begin{aligned} F_{T_{cho}}(t) &= \Pr(T_{cho} \le t) \\ &= \int_0^{\infty}\int_0^{\infty} \Pr(T_{cho} \le t | T_t = \tau_1, T_s = \tau_2) \\ &\quad \times dF_{T_t}(\tau_1)dF_{T_s}(\tau_2) \\ &= F_{T_{ch}}(t) + F_{T_t}(t) + F_{T_s}(t) \\ &\quad - F_{T_{ch}}(t)F_{T_t}(t) - F_{T_{ch}}(t)F_{T_{sh}}(t) \\ &\quad - F_{T_t}(t)F_{T_s}(t) + F_{T_{ch}}(t)F_{T_t}(t)F_{T_s}(t). \end{aligned} \tag{11}$$

Finally, the mean channel holding time can be expressed as

$$E[T_{cho}] = \int_0^{\infty} (1 - F_{T_{cho}}(t))\, dt. \tag{12}$$

Fig. 5 compares analytical approximated results of (7) with simulation results of (6) for $E[T_{ch}] = 100$ s, $M = 10$, $P_s = 0.5$, and $r = 5$. The results agree in terms of the mean channel holding time. Therefore, the approximation of (7) is acceptable.

B. Call Arrival Rate

Four different types of calls exist in this system; new, straight-handoff, turning-handoff, and intracell-handoff calls. Handoff

calls are generated from a Poisson arrival of new calls and approximate another Poisson process. Therefore, the total call arrival rate is represented by the sum of each arrival rate

$$\lambda = \lambda_n + \lambda_{sh} + \lambda_{th} + \lambda_{ih} \tag{13}$$

where λ_{sh}, λ_{th}, and λ_{ih} denote the arrival rate of straight-handoff, turning-handoff, and intracell-handoff calls, respectively.

Turning-handoff and intracell-handoff calls are assumed to be evenly distributed over all microzones while straight-handoff calls are generated only at the ends of a cigar-shaped cell (i.e., the first and Mth microzones). The call arrival rate of each microzone can be written as

$$\lambda_j = \begin{cases} \dfrac{\lambda_n + \lambda_{th} + \lambda_{ih}}{M} + \dfrac{\lambda_{sh}}{2}, & j = 1 \text{ or } M \\ \dfrac{\lambda_n + \lambda_{th} + \lambda_{ih}}{M}, & 2 \le j \le M-1. \end{cases} \tag{14}$$

Let P_{sh_j}, P_{th_j}, and P_{ih_j} denote the probabilities that a call generated in the jth microzone causes straight handoff, turning handoff, and intracell handoff, respectively. Then, λ_{sh}, λ_{th}, and λ_{ih} are given by

$$\lambda_{sh} = \sum_{j=1}^{M} \lambda_j (1 - P_b) P_{sh\_j} \tag{15}$$

$$\lambda_{th} = \sum_{j=1}^{M} \lambda_j (1 - P_b) P_{th\_j} \tag{16}$$

$$\lambda_{ih} = \sum_{j=1}^{M} \lambda_j (1 - P_b) P_{ih\_j} \tag{17}$$

where P_b is the blocking probability. The probabilities P_{sh_j}, P_{th_j}, P_{ih_j}, and P_b are obtained in Section III-D.

C. System State Probability

The system state S denotes the number of callers in a cigar-shaped cell. The maximum state is constrained by the number of channel elements installed in the system and is given by

$$S_{\max} = \gamma \times N. \tag{18}$$

The proposed system can be modeled as an $M/G/S_{\max}$ loss system with a Poisson call arrival (**M**emoryless property of inter-arrival time), a **G**enerally distributed call service time, a finite system capacity with $S_{\max}$ servers and blocked calls (call **loss**). The limiting distribution of the system is identical to that of an $M/M/S_{\max}$ loss system with an exponentially distributed call service time due to the *insensitivity property* [17]. A state transition diagram is shown in Fig. 6. In this figure, $P_b^{(s)}$ is the blocking probability at state s. From balance equations, the system state probability is obtained as

$$P(s) = \begin{cases} \dfrac{1}{s!}\left(\dfrac{\lambda}{\mu}\right)^s P(0), & 0 \le s \le N \\ \dfrac{1}{s!}\left(\dfrac{\lambda}{\mu}\right)^s \displaystyle\prod_{k=N}^{s-1} \left(1 - P_b^{(k)}\right) P(0), & N < s \le S_{\max} \end{cases} \tag{19}$$

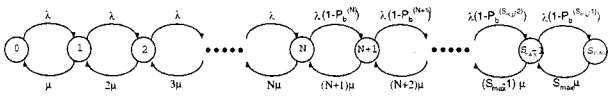

Fig. 6. State transition diagram.

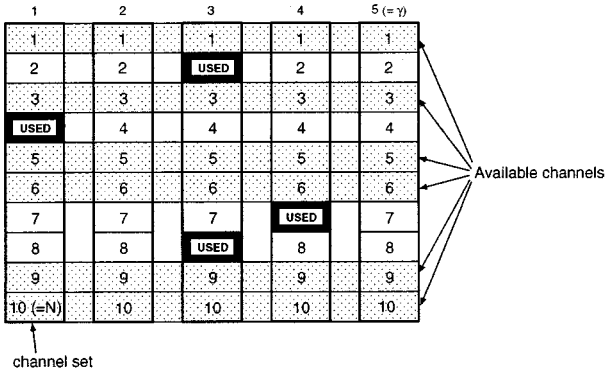

Fig. 7. An example of the channel assignment state of a home microzone for $N = 10$, $\gamma = 5$, and $\sigma_{ho} = 4$.

where

$$P(0) = \left[\sum_{k=0}^{N} \frac{1}{k!}\left(\frac{\lambda}{\mu}\right)^k + \sum_{k=N+1}^{S_{\max}} \frac{1}{k!}\left(\frac{\lambda}{\mu}\right)^k \prod_{i=N}^{k-1}\left(1 - P_b^{(i)}\right)\right]^{-1},$$

$$\mu = \frac{1}{E[T_{cho}]}.$$

D. Blocking, Dropping and Handoff Attempt Probabilities

Let the local system state σ denote the number of callers in a microzone. Then, $0 \le \sigma \le N$. The local state that a new call encounters at the home microzone is denoted by σ_{ho}, and the local state that an intracell-migration call encounters at the entrance to a target microzone is denoted by σ_{in}.

Fig. 7 shows an example of the channel assignment state of a home microzone at the instant of a new call generation for $N = 10$, $\gamma = 5$, and $\sigma_{ho} = 4$. A new call for $\sigma_{ho} = k$ and $S = s$ is blocked if each of all available channels of $N - k$ in a home microzone is commonly occupied by γ users outside the home microzone. Let

$$\begin{aligned} L &= N\gamma - k \\ W &= s - k \\ U &= (N - k)\gamma \end{aligned}$$

where L, W, and U represent the number of channel elements not used in the home microzone, the number of callers outside the home microzone, and the number of channel elements available in the home microzone, respectively. Then, the blocking probability under the conditions of $S = s$ and $\sigma_{ho} = k$ is obtained as

$$\begin{aligned} P_b^{(s,k)} &= \Pr(\text{blocking} | S = s,\ \sigma_{ho} = k) \\ &= \begin{cases} \dfrac{\binom{L-U}{W-U}}{\binom{L}{W}}, & U \le W \\ 0, & \text{otherwise.} \end{cases} \end{aligned} \tag{20}$$

Removing the condition of σ_{ho} with probability law yields the blocking probability

$$P_b^{(s)} = \sum_{k=0}^{N} P_b^{(s,k)} \Pr(\sigma_{ho} = k). \tag{21}$$

The probability that σ_{ho} is k is given by

$$\Pr(\sigma_{ho} = k) = \frac{{}_{M-1}H_{s-k} - \sum_{i=1}^{I'} (-1)^{i+1} \binom{M-1}{i} {}_{M-1}H_{s-k-i(N+1)}}{{}_{M}H_{s} - \sum_{i=1}^{I} \binom{M}{i} (-1)^{i+1} {}_{M}H_{s-i(N+1)}} \tag{22}$$

where I and I' are the largest integers i such that $s-i(N+1) \geq 0$ and $s-k-i(N+1) \geq 0$, respectively, and

$${}_aH_b = \binom{a+b-1}{b}.$$

Finally, the blocking probability is expressed as

$$P_b = \sum_{s=1}^{S_{\max}} P(s) P_b^{(s)}. \tag{23}$$

An intracell migration call requires handoff if the migrating channel is already occupied by someone in the target microzone. The probability that an intracell migration call requests handoff for $S = s$ is given by

$$P_{hr}^{(s)} = \sum_{k=0}^{N} \frac{k}{N} \Pr(\sigma_{in} = k). \tag{24}$$

An intracell migration call fails and the call is incompletely terminated for $\sigma_{in} = k$ and $S = s$ if the migrating channel is already occupied by someone in the target microzone and if each of all available channels of $N-k$ in the target microzone is commonly occupied by γ users outside the target microzone. Similarly to the case of blocking, the intracell migration failure probability under the conditions of $S = s$ and $\sigma_{in} = k$ is obtained as

$$P_{mf}^{(s,k)} = \Pr(\text{intracell migration failure} | S = s, \sigma_{in} = k) = \begin{cases} \dfrac{\binom{L-1-U}{W-1-U}}{\binom{L-1}{W-1}} \dfrac{k}{N}, & U \leq W-1 \\ 0, & \text{otherwise.} \end{cases} \tag{25}$$

The intracell migration failure probability is derived by removing the condition of σ_{in} as

$$P_{mf}^{(s)} = \sum_{k=0}^{N} P_{mf}^{(s,k)} \Pr(\sigma_{in} = k). \tag{26}$$

For any k it is more likely that σ_{in} is k when the number of callers outside the target microzone is larger rather than smaller, which is known as an *inspection paradox* [17]. From this, the probability that σ_{in} is k is obtained as

$$\Pr(\sigma_{in} = k) = \frac{(s-k) \Pr(\sigma_{ho} = k)}{\sum_{i=0}^{N} (s-i) \Pr(\sigma_{ho} = i)}. \tag{27}$$

Finally, the intracell migration failure probability is given by

$$P_{mf} = \sum_{s=1}^{S_{\max}} P(s) P_{mf}^{(s)}. \tag{28}$$

A call may be dropped incompletely within a cell due to an intracell migration failure. The probability that a call generated in the jth microzone in a cigar-shaped cell is eventually dropped within a cell due to an intracell migration failure is written as

$$P_{d\_j} = P_{\text{short}} \sum_{i=1}^{j-1} \Pr\left(T_{ch} > T_{dw}^{(i)}\right) P_s^i (1-P_{mf})^{i-1} P_{mf} + P_{\text{long}} \sum_{i=1}^{M-j} \Pr\left(T_{ch} > T_{dw}^{(i)}\right) P_s^i (1-P_{mf})^{i-1} P_{mf} \tag{29}$$

where

$$\begin{aligned} \Pr\left(T_{ch} > T_{dw}^{(i)}\right) &= \int_0^{\infty} (1 - F_{T_{ch}}(t)) f_{T_{dw}^{(i)}}(t)\, dt \\ &= \int_0^{\infty} \exp(-\mu_{ch} t) \cdot \frac{r\mu_{dw} (r\mu_{dw} t)^{ir-1}}{(ir-1)!} \\ &\quad \times \exp(-r\mu_{dw} t)\, dt \\ &= \left[\frac{r\mu_{dw}}{\mu_{ch} + r\mu_{dw}}\right]^{ir} \end{aligned}$$

and P_{short} and P_{long} are the probabilities of moving toward the nearer and farther cell boundaries from the call generation point, respectively. Therefore, the dropping probability is obtained as

$$P_d = \frac{1}{M} \sum_{j=1}^{M} P_{d\_j}. \tag{30}$$

Similarly, the probability that a call generated in the jth microzone requests intracell handoff is given by

$$P_{ih\_j} = P_{\text{short}} \sum_{i=1}^{j-1} \Pr\left(T_{ch} > T_{dw}^{(i)}\right) P_s^i (1-P_{hr})^{i-1} P_{hr} + P_{\text{long}} \sum_{i=1}^{M-j} \Pr\left(T_{ch} > T_{dw}^{(i)}\right) P_s^i (1-P_{hr})^{i-1} P_{hr} \tag{31}$$

TABLE I
LIST OF SYSTEM PARAMETERS

Average call holding time, $E[T_{ch}]$	100 s
Average dwelling time in a microzone, $E[T_{dw}^{(1)}]$	500 s
Stage of Erlang distribution, r	5
P_{short}, P_{long} and P_s	0.5
Number of microzones in a cigar-shaped cell, M	10
Number of channel sets in CS, γ	5
Number of channel elements in a channel set, N	7

where $P_{hr} = \sum_{s=1}^{S_{\max}} P(s)P_{hr}^{(s)}$. The probabilities P_{sh_j} and P_{th_j} mentioned in Section III-B are also expressed as

$$P_{sh\_j} = P_{\text{short}} \Pr\left(T_{ch} > T_{dw}^{(j)}\right) P_s^j (1-P_{mf})^{j-1} + P_{\text{long}} \Pr\left(T_{ch} > T_{dw}^{(M-j+1)}\right) \times P_s^{M-j+1}(1-P_{mf})^{M-j} \quad (32)$$

$$P_{th\_j} = P_{\text{short}} \sum_{i=1}^{j} \Pr\left(T_{ch} > T_{dw}^{(i)}\right) P_s^{i-1}(1-P_s) \times (1-P_{mf})^{i-1} + P_{\text{long}} \sum_{i=1}^{M-j+1} \Pr\left(T_{ch} > T_{dw}^{(i)}\right) \times P_s^{i-1}(1-P_s)(1-P_{mf})^{i-1}. \quad (33)$$

IV. NUMERICAL EXAMPLES

System performance is evaluated with numerical results obtained by an iteration method in which P_b and λ are interdependent. Low-tier user characteristics in urban microcellular environments are considered in choosing the values of system parameters; frequent stopping for shopping, waiting for a bus or a taxi, calling, and so on. We assumed that average dwelling time in a microzone is 500 s and a stage of Erlang distribution, r is 5; an Erlang distribution with r larger than 5 has a density function similar to that of a normal distribution. Number of microzones, channel sets, and channel elements per channel set are chosen among reasonable values to make the blocking probability within such a range as $10^{-4} < P_b < 10^{-1}$. The parameters used in the numerical examples are summarized in Table I.

Fig. 8 shows blocking and dropping probabilities versus traffic load. The proposed system accommodates a traffic load of 14 Erlangs under the condition of 7 channels with a blocking probability of 1%. A conventional system, i.e., a system with no channel-reuse within a cell, handles only 2.5 Erlangs under the same conditions (Erlang loss formula). This result corresponds to a system capacity increase up to 560% (=14/2.5). This increase in system capacity is significant. On the other hand, call dropping caused by intracell migration failures within a cell is insignificant when compared with the call blocking. The dropping probability is maintained below 0.01% until the traffic load reaches 14 Erlangs for a blocking probability of 1%.

Fig. 9 shows the handoff call arrival rates for turning, straight, and intracell handoff versus the new call arrival rate. The turning handoff rate is dominant. The proposed system may generate additional intracell handoff calls which can cause an increase in the signaling traffic load. As shown in Fig. 9, however, the increase

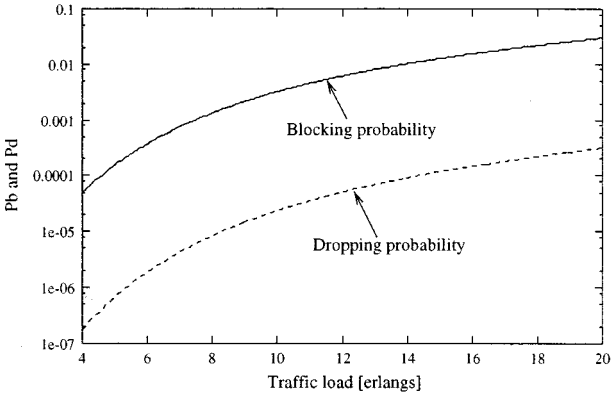

Fig. 8. Blocking and dropping probabilities.

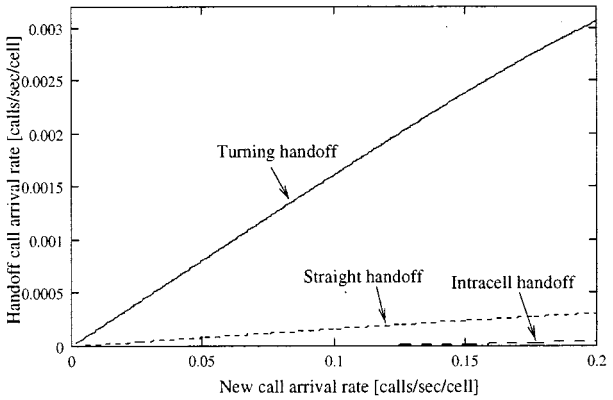

Fig. 9. Handoff call arrival rates.

in the number of intracell handoff calls is negligible when compared with the number of turning and straight handoff calls.

In this analysis the average reuse index is derived as

$$\overline{\eta} = \frac{\sum_{s=1}^{S_{\max}} sP(s)}{N} \quad (34)$$

where $\overline{\eta}$ represents how many times a channel is reused (on average) in a cell.

Fig. 10 shows the average reuse index versus the traffic load. As traffic load increases, $\overline{\eta}$ increases toward a value of γ. When the traffic load is 14 Erlangs for a blocking probability of 1%, $\overline{\eta}$ is 1.98, which means 13.86 ($=1.98 \times N$) independent channels are fully used. This value is in agreement with the carried load of 13.86 ($=14 \times 0.99$) Erlangs.

The movable safety zone (MSZ) scheme proposed by Cho *et al.* [11] reuses a radio channel every other microzone in a cigar-shaped cell. Fig. 11 compares the proposed system in this paper to the MSZ scheme in terms of a weighted sum $P_b+10{\cdot}P_d$. For a light traffic load below an average reuse index of 1, the performance of both systems is nearly identical because the effect of channel reuse does not appear. On the other hand, for a heavy traffic load the proposed system yields better performance than the MSZ scheme because the reuse efficiency of the proposed system is higher than for the MSZ scheme. As traffic load increases the performance difference becomes greater. With a performance index, $P_b + 10 \cdot P_d$ of 1% the proposed system can

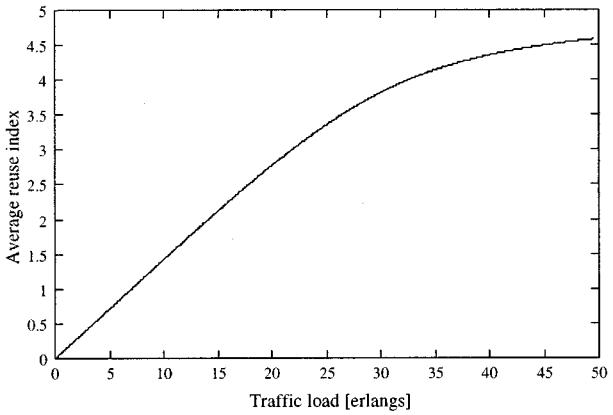

Fig. 10. Average reuse index.

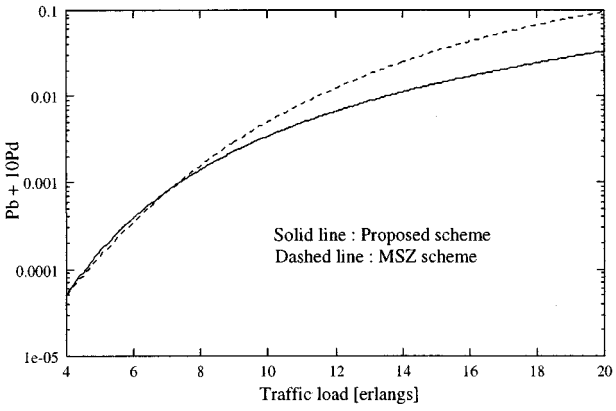

Fig. 11 Comparison between the proposed system and the MSZ scheme in terms of $P_b + 10 \cdot P_d$.

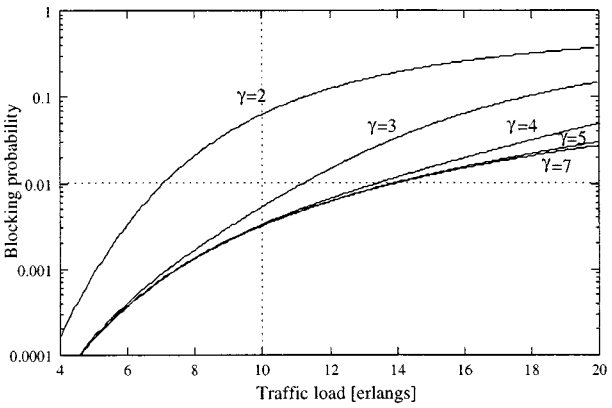

Fig. 12. Blocking probability for varying γ.

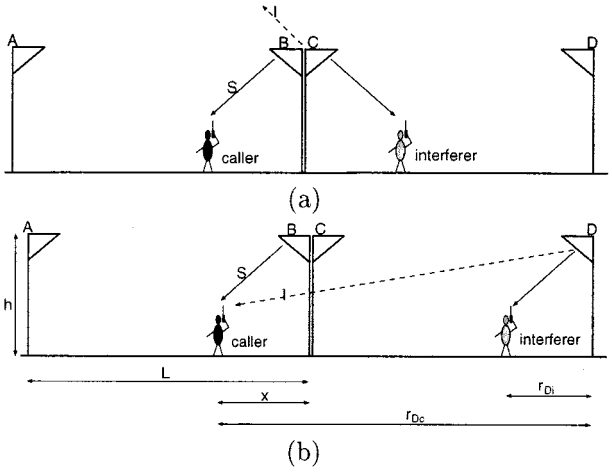

Fig. 13. Cochannel interference on forward link: (a) through a back-lobe beam and (b) through a main-lobe beam.

handle approximately 13.6 Erlangs while the MSZ scheme handles 11.5 Erlangs.

The hardware cost for installing channel elements is important. Installation of too many channel sets is expensive and the improvement in performance may not justify the cost. Therefore, a minimum value of γ satisfying the required quality of services (QoS) needs to be determined. Fig. 12 shows the blocking probability for varying the value of γ. Performance improvement obtained by an increase in γ is significant when γ is smaller than 4. It is insignificant when γ is larger than 4. For a cell area with a traffic load of 10 Erlangs the optimum value of γ is 3 for a blocking probability of 1%.

V. Conclusion

A new microcell configuration is proposed in which directional-beam antennas are located along streets in order to manage multiple noninterfered microzones within a cigar-shaped cell. The system can simultaneously use a radio channel in multiple microzones adjoining each other, resulting in increased reuse efficiency of radio resources, thereby significantly increasing system capacity.

The proposed system is evaluated with numerical examples in terms of blocking and dropping probabilities, handoff call arrival rate, and channel reuse index. The examples show that the proposed system increases system capacity up to 560% when compared with a conventional system. The number of channel elements installed in a CS needs to be determined by considering both system performance and hardware cost.

Appendix

We validate that a traffic channel can overcome cochannel interference induced from adjoining microzones and therefore can be used concurrently in multiple microzones within a cell. We derived the signal-to-interference ratio on both forward and reverse links based on previous works [18]–[20].

A. Forward Link

Fig. 13 illustrates how a caller is interfered by a cochannel user interferer staying in an adjoining microzone on forward link. If an interferer approaches the antenna C, as shown in the Fig. 13(a), interference is given to the caller through the back-lobe beam of antenna C. The strength of the back-lobe beam is weaker than a main-lobe beam by 20–30 dB [21]. In addition, the back-lobe beam should be up-tilted in this system, which makes the signal strength to the caller in ground much weaker. Therefore, interference caused by an interferer staying in the region of antenna C is negligible. On the other hand, a cochannel user staying near to antenna D, as shown in Fig. 13(b) interferes with a call via the main-lobe beam of antenna D. Assuming a perfect power control, it is noted that the strongest

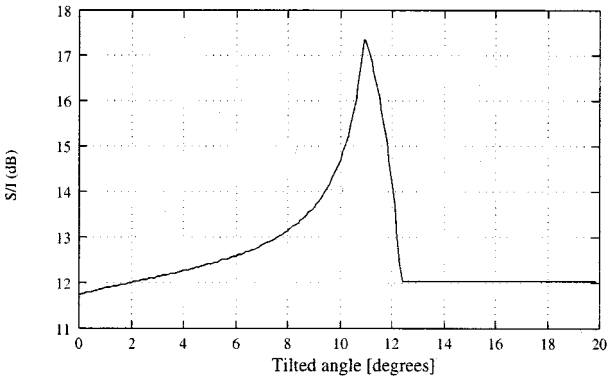

Fig. 14. S/I versus the tilted beam angle on forward link ($h = 5$ m and $L = 200$ m).

signal is transmitted when an interferer is located at $L/2$ from the antenna D, where L is the distance of a microzone between two antennas. Therefore, the worst case of signal-to-interference ratio (S/I) occurs when an interferer is located at a distance of $L/2$ from the antenna D. We will show that the signal-to-interference ratio in the worst case is higher than 12 dB which satisfies the requirement in digital mobile communication systems [22]. An antenna with a tilted-beam has a gain [13]

$$G = \begin{cases} 1 - (\varphi/BW)^2, & 0 \le \varphi \le (BW - 0.5^\circ) \\ 0.1, & \text{otherwise,} \end{cases} \tag{35}$$

where the angle BW is assumed to be 10° and φ is the angle between the direction of a tilted-beam and the direction from the antenna to a user. In Fig. 13(b) the signal strength that the caller receives from antenna B is assumed to be the same as that the interferer receive from antenna D because of the previous assumption of the perfect power control. Therefore, the signal strength received by the caller is obtained as

$$S = P_D \times G_i \times L_{D_i} \tag{36}$$

where

P_D is the transmitted power from antenna D,
G_i is the gain of antenna D to the interferer, and
L_{D_i} is the path loss from antenna D to the interferer.

On the other hand, the interference to the caller is expressed as

$$I = P_D \times G_c \times L_{D_c} \tag{37}$$

where G_c is the gain of antenna D to the caller and L_{D_c} is the path loss from antenna D to the caller. It is assumed that the value of path loss exponent is 4. Then, the signal to interference ratio is given by

$$S/I = \frac{G_i \times r_{D_i}^{-4}}{G_c \times r_{D_c}^{-4}} \tag{38}$$

where r_{D_i} and r_{D_c} are the distances from antenna D to the interferer and to the caller, respectively.

Fig. 14 shows the signal-to-interference ratio versus the tilted beam angle when the antenna height, h and the distance between two antennas, L are 5 m and 200 m, respectively. The optimum value of tilted angle is 10.93° at which S/I is the largest, and this S/I result is improved by 5.62 dB compared to a nontilted-beam system. The S/I ratio does not depend on the tilted angle if the tilted angle exceeds 12.3° because both the caller and the interferer are out of the main-lobe beam. Several results on S/I improvement for three different cases of h and L are shown in Table II.

TABLE II
S/I IMPROVEMENTS DUE TO ANTENNA TILTING ON FORWARD LINK

antenna height, h (m)	5	5	8
distance between antennas, L (m)	200	100	100
resulting S/I (dB)	17.36	19.40	20.62
S/I improvement (dB)	5.62	8.77	15.33

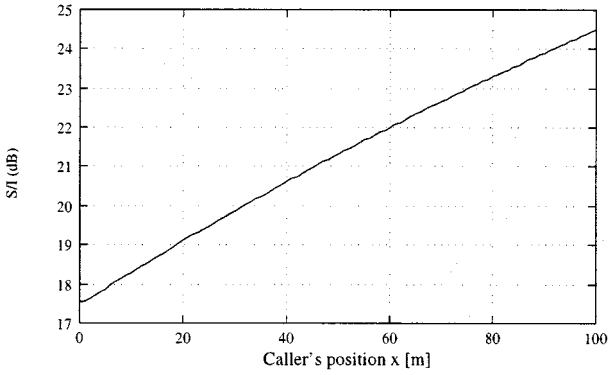

Fig. 15. S/I at the caller's position x ($h = 5$ m, $L = 200$ m, and the tilted angle = 10.93°).

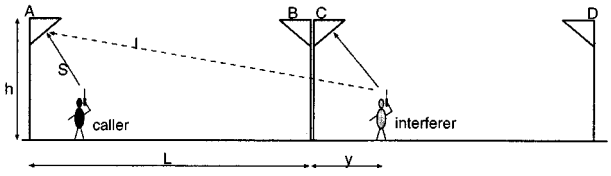

Fig. 16. Cochannel interference on reverse link.

Fig. 15 shows the signal-to-interference ratio at the caller's position x which is limited to $L/2$, 100 m in this example, because both the signal and interference features are symmetrical at the center of a microzone. The minimum value of S/I is approximately 17.5 dB at $x = 0$, which is much higher than the required values of S/I in digital wireless communication systems [22].

B. Reverse Link

Similarly to the case of forward link, the S/I ratio can be obtained on reverse link. Fig. 16 shows an example of the call interfered by a cochannel user staying in an adjoining microzone on reverse link. Under the assumption of a perfect power control, the signal strength S received at antenna A is constant independent of caller's position. The S/I is only determined by the interferer's position y. Fig. 17 shows the S/I ratio versus y under the same conditions on the forward link. Passing through the point P, the interferer is getting out of the main-lobe beam of antenna A, and therefore, the S/I value temporally increases. The S/I on reverse link also shows symmetrical features at the center of a microzone. The minimum value of S/I at $y = 100$ m also satisfies the requirement in digital wireless communication systems.

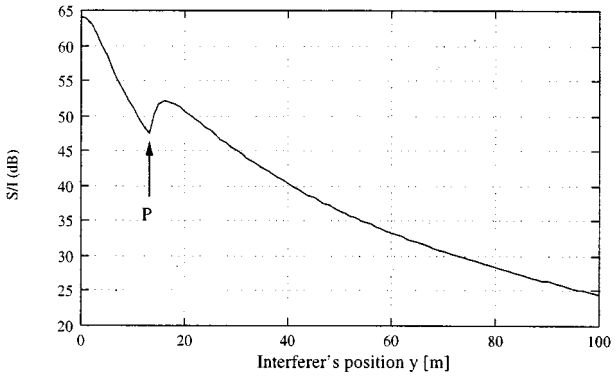

Fig. 17. S/I at the interferer's position y ($h = 5$ m, $L = 200$ m, and the tilted angle $=10.93°$).

In summary, on both forward and reverse links the S/I values are kept at acceptable level even when a cochannel user stays in the adjoining microzone.

REFERENCES

[1] J. Chuang, "Performance issues and algorithms for dynamic channel assignment," *IEEE J. Select. Areas Commun.*, vol. 11, pp. 955–963, Aug. 1993.

[2] S. Yasuda and S. Onoe, "Autonomous channel assignment control for flexible reuse in mobile radio systems," in *Proc. IEEE VTC*, 1992, pp. 798–801.

[3] K. N. Chang, J. T. Kim, C. S. Yim, and S. Kim, "An efficient borrowing channel assignment scheme for cellular mobile systems," *IEEE Trans. Veh. Technol.*, vol. 47, pp. 602–608, 1998.

[4] J. L. Pan, P. M. Djuric, and S. S. Rappaport, "Multibeam cellular communication systems with dynamic channel assignment," in *Proc. IEEE VTC*, 1998, pp. 2140–2144.

[5] H. S. Cho and D. K. Sung, "Performance improvement of cross-shaped urban microcellular systems with switched-beam antennas," in *Proc. IEEE Globecom*, 1998, pp. 3209–3214.

[6] J. Shapira, "Microcell engineering in CDMA cellular networks," *IEEE Trans. Veh. Technol.*, vol. 43, pp. 817–825, 1994.

[7] M. V. Clark, V. Erceg, and L. J. Greenstein, "Reuse efficiency in urban microcellular networks," *IEEE Trans. Veh. Technol.*, vol. 46, pp. 279–288, 1997.

[8] T. S. Chu and M. J. Gans, "Fiber optic microcellular radio," *IEEE Trans. Veh. Technol.*, vol. 40, pp. 599–606, Aug. 1991.

[9] H. Ichikawa and M. Ogasawara, "A centralized control microcell radio system with spectrum delivery switches," *IEICE Trans. Commun.*, vol. E76-B, no. 9, pp. 1115–1121, Sept. 1993.

[10] J.-S. Wu, J. Wu, and H.-W. Tsao, "A radio-over-fiber network for microcellular system application," *IEEE Trans. Veh. Technol.*, vol. 47, pp. 84–94, Feb. 1998.

[11] H. S. Cho, S. H. Kang, and D. K. Sung, "A movable safety zone scheme in urban fiber-optic microcellular systems," *IEEE Trans. Veh. Technol.*, vol. 48, pp. 1099–1109, July 1999.

[12] D. J. Y. Lee and C. Xu, "Mechanical antenna downtilt and its impact on system design," in *Proc. IEEE VTC*, Phoenix, USA, 1997, pp. 447–451.

[13] J.-S. Wu, J.-K. Chung, and C.-C. Wen, "Hot-spot traffic relief with a tilted antenna in CDMA cellular networks," *IEEE Trans. Veh. Technol.*, vol. 47, pp. 1–9, Feb. 1998.

[14] H. S. Cho and D. K. Sung, "Channel holding time distribution in cross- and cigar-shaped urban microcells," *IEICE Trans. Commun.*, vol. E81-B, no. 6, pp. 1275–1279, June 1998.

[15] T. E. Darcie, "Subcarrier multiplexing for multiple-access lightwave networks," *J. Lightwave Technol.*, vol. LT-5, pp. 1103–1110, Aug. 1987.

[16] R. Ohmoto, H. Ohtsuka, and H. Ichikawa, "Fiber-optic microcell radio systems with a spectrum delivery scheme," *IEEE J. Select. Areas Commun.*, vol. 11, pp. 1108–1117, Sept. 1993.

[17] R. W. Wolff, *Stochastic Modeling and the Theory of Queues*. Englewood Cliffs, NJ: Prentice-Hall, 1989.

[18] J. B. Andersen, T. S. Rappaport, and S. Yoshida, "Propagation measurements and models for wireless communications channels," *IEEE Commun. Mag.*, vol. 33, pp. 42–49, Jan. 1995.

[19] H. H. Xia, H. L. Bertoni, L. R. Maciel, A. Lindsay-Stewart, and R. Rowe, "Microcellular propagation characteristics for personal communications in urban and suburban environments," *IEEE Trans. Veh. Technol.*, vol. 43, pp. 743–752, Aug. 1994.

[20] M. J. Feuerstein, K. L. Blackard, T. S. Rappaport, S. Y. Seidel, and H. H. Xia, "Path loss, delay spread, and outage models as functions of antenna height for microcellular system design," *IEEE Trans. Veh. Technol.*, vol. 43, pp. 487–498, Aug. 1994.

[21] M. F. Catedra and J. Perez-Arriaga, *Cell Planning for Wireless Communications*. New York: Artech House, 1999.

[22] W. C. Y. Lee, "Spectrum efficiency in celluar," *IEEE Trans. Veh. Technol.*, vol. 38, pp. 69–75, May 1989.

Ho-Shin Cho (S'92–M'00) received the B.S., M.S., and Ph.D. degrees in electrical engineering from the Korea Advanced Institute of Science and Technology (KAIST), in 1992, 1994, and 1999, respectively.

Since March 1999, he has been a Senior Member of Technical Staff with the Electronics and Telecommunications Research Institute (ETRI), where he has conducted studies on performance analysis and test of base station for IMT-2000. His research interests include mobility modeling, resource allocation,traffic analysis, and intelligent antenna scheme in wireless communication systems.

Jae Kyun Kwon (S'96) received the B.S. and M.S. degrees in electrical engineering from the Korea Advanced Institute of Science and Technology (KAIST), in 1996 and 1998, respectively. He is currently working toward the Ph.D. degree in electrical engineering at KAIST.

His research interests include mobile communication networks, CDMA soft handoff, and mobility modeling.

Dan Keun Sung (S'80–M'86) received the B.S. degree in electrical engineering from Seoul National University, in 1975, and the M.S. and Ph.D. degrees in electrical and computer engineering from the University of Texas at Austin, in 1982 and 1986, respectively.

From May 1977 to July 1980, he was a Research Engineer with the Electronics and Telecommunications Research Institute where he had been engaged in research on the developement of electronic switching systems. In 1986, he joined the faculty of the Korea Institute of Technology and is currently Professor of Dept. of Electrical Engineering at the Korea Advanced Institute of Science and Technology (KAIST). His research interests include ATM switching systems, wireless networks, intelligent network performance and reliability of systems, mobile communication systems, wireless ATM, and CDMA system. He is a member of IEICE, KITE, KICS, and KISS.